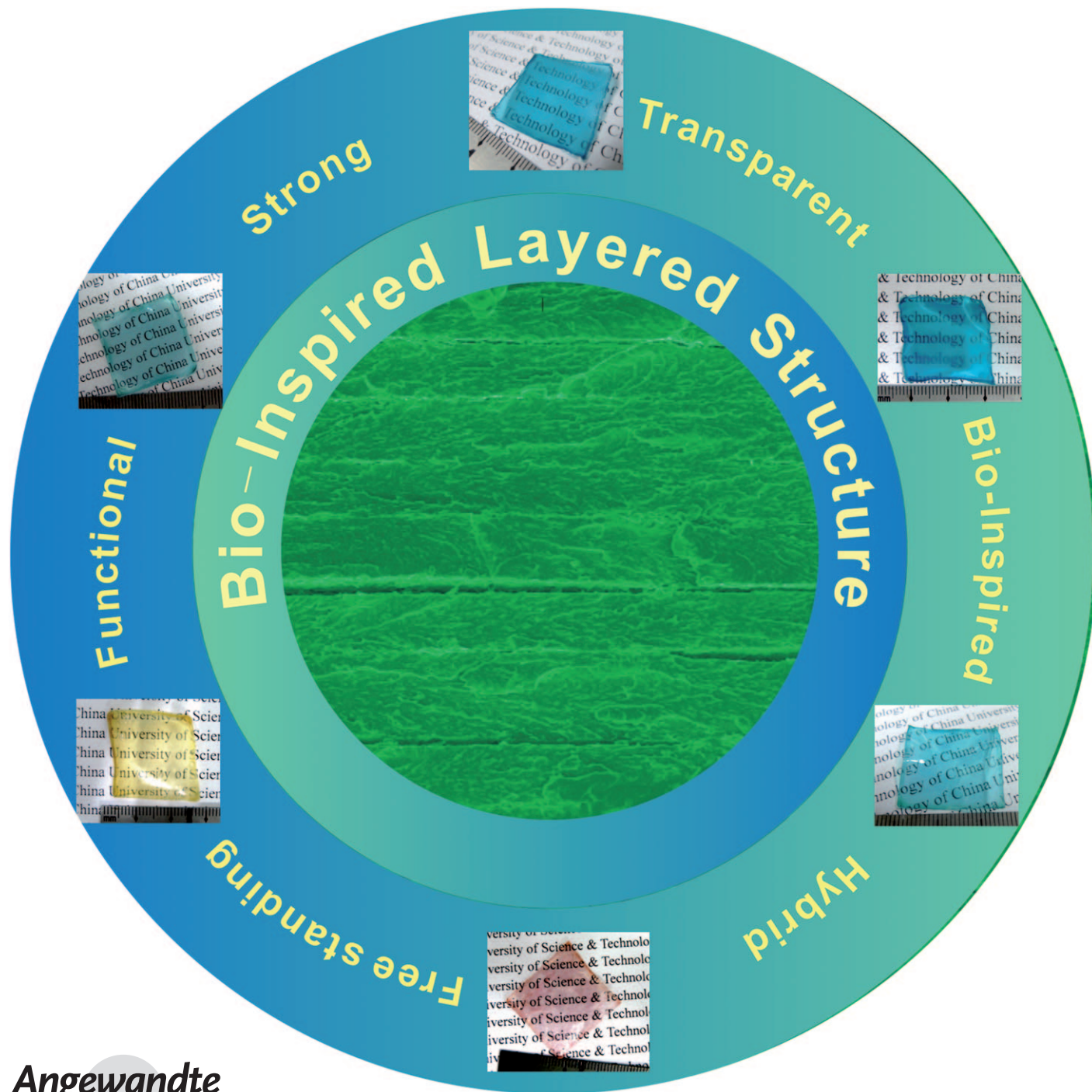


# Biologically Inspired, Strong, Transparent, and Functional Layered Organic–Inorganic Hybrid Films\*\*

Hong-Bin Yao, Hai-Yu Fang, Zhi-Hua Tan, Li-Heng Wu, and Shu-Hong Yu\*



Angewandte  
Chemie

In the field of advanced materials design, good mechanical performance and multifunctionality are highly desirable and can often be realized through unique hybrid structures or composite materials. Strategies for materials design are highly multidisciplinary; just as the designed models in materials engineering are necessary to achieve excellent mechanical properties, the functional design of materials needs chemical or biological knowledge for the modification of materials. Surprisingly, in the process of evolution, nature has found a way to produce light-weight, strong, and high-performance materials with exceptional properties and functionalities by synergistically combining the models, methods, and approaches of materials engineering, chemistry, and biology. For example, seashell nacre and bones are well known for their hardness, strength, and toughness (superior to many synthetic ceramics and composites<sup>[1]</sup>) complemented by unique biological and biomedical properties.<sup>[2]</sup> These natural materials consist of brittle biominerals connected by a small amount of protein and have highly sophisticated structures with complex hierarchical designs whose properties far exceed what could be expected from a simple mixture of their components.<sup>[3]</sup>

Continuing attention has been paid to the systematic study of natural materials<sup>[4]</sup> with the objective of duplicating their properties in artificial materials.<sup>[5]</sup> A number of different inorganic platelets including glass, graphite, silicon carbide, and clays have been used as fillers dispersed randomly into polymer matrixes for the fabrication of artificial composite materials.<sup>[6]</sup> The strength, hardness, and stiffness of these composites were enhanced compared to the pure polymer matrix or inorganic phase, but the improvement is still notably smaller than that realized by natural materials and that expected by theoretical models for reinforced polymers.

Recently, innovative techniques have been used to fabricate artificial composites by mimicking the micro- and nanostructures of natural materials. The mechanical performance of the obtained artificial materials is equal to or even better than that of natural materials. For example, layer-by-layer (LBL) deposition of polyelectrolyte and clay platelets was used to fabricate a nanostructured artificial nacre.<sup>[7]</sup> Cross-linking of LBL-deposited poly(vinyl alcohol)/mont-

morillonite nanocomposites yielded materials with tensile strengths up to 400 MPa, which are stronger than the natural nacre.<sup>[8]</sup> The microscopic layers formed by ice crystals were also used as a template for a fine ceramic structure, which could then be infiltrated with softer materials to build complex microstructured composites.<sup>[9]</sup> The Al<sub>2</sub>O<sub>3</sub>/poly-(methyl methacrylate) composite with “brick-and-mortar” structure fabricated by this ice template crystallization method is 300 times tougher than its constituents.<sup>[10]</sup> Furthermore, the spin-coating technique was used in the fabrication of lamellar alumina/chitosan hybrid films with high flaw tolerance and ductility.<sup>[11]</sup>

Platelet-like inorganic building blocks are essential elements in the biomimetic fabrication of novel artificial composites, especially those aiming to recreate a biologically inspired layered “brick-and-mortar” micro- and nanostructure. However, in previous reports, the natural clay minerals and ceramic Al<sub>2</sub>O<sub>3</sub> platelets used to make composites with biologically inspired structures<sup>[7–11]</sup> just reinforced the polymer matrix without bringing other functionalities to these artificial composites. Herein, we use functional inorganic platelets to fabricate artificial organic–inorganic hybrid films with biologically inspired structures. In this way, the materials not only achieve high strength but are also simultaneously endowed with other special functionalities. The layered double hydroxides (LDHs), which can be represented by the general formula  $[M^{2+}_{1-x}M^{3+}_x(OH)_2][A^{m-}]_{x/m} \cdot nH_2O$  (see the general structure in Figure 1a), were chosen as the building blocks for fabricating biologically inspired, strong, and functional organic–inorganic hybrid films, as LDHs exhibit interesting optical,<sup>[12]</sup> catalytic,<sup>[13]</sup> magnetic,<sup>[14]</sup> and fire-retardant properties.<sup>[15]</sup> More importantly, these LDH platelets could be synthesized on a large scale by simple chemical precipitation.<sup>[14b,16]</sup> Although some studies have been conducted on the application of LDHs in composites,<sup>[17]</sup> using LDH platelets as the inorganic bricks in the fabrication of biologically inspired organic–inorganic hybrid films has been rarely reported.

LDH micro- and nanoplatelets of Cu<sub>2</sub>(OH)<sub>3</sub>NO<sub>3</sub> (Cu-NO<sub>3</sub>),  $[Co_{0.67}Al_{0.33}(OH)_2][(CO_3)_{0.165} \cdot 0.49H_2O]$  (Co-Al-CO<sub>3</sub>), and Eu(OH)<sub>2.5</sub>Cl<sub>0.5</sub>·0.8H<sub>2</sub>O (Eu-Cl) were synthesized by slightly modified approaches according to published methods (see the Supporting Information, Part II).<sup>[12a,18]</sup> PXRD patterns of these LDH platelets are shown in Figure 1b, which indicates that as-synthesized micro- and nanoplatelets are pure phases. These platelets adopt layered structures with a series of *00l* diffraction peaks. Because of the intrinsically layered symmetry in the crystal structure (Figure 1a), the LDH crystals prefer to grow into platelet-like morphologies, thus making them useful building blocks in the fabrication of layered organic–inorganic hybrid materials. The morphologies of the obtained Cu-NO<sub>3</sub>, Co-Al-CO<sub>3</sub>, and Eu-Cl crystals were characterized by scanning electron microscopy (SEM; Figure 1c–h). All of them display platelet-like micro- and nanomorphologies with a mean lateral size of 10–20, 3–4, and 1 μm and a thickness of 200, 100, and 10 nm, respectively.

In a first step, slightly hydrophobic amine-terminated silane species were attached to the surfaces of as-synthesized LDH platelets to achieve self-assembly of the colloidal

[\*] H. B. Yao, H. Y. Fang, Z. H. Tan, L. H. Wu, Prof. Dr. S. H. Yu  
Division of Nanomaterials and Chemistry  
Hefei National Laboratory for Physical Sciences at Microscale  
Department of Chemistry  
University of Science and Technology of China  
Hefei, Anhui 230026 (China)  
Fax: (+86) 551-360-3040  
E-mail: shyu@ustc.edu.cn

[\*\*] S.H.Y. acknowledges the funding support from the National Basic Research Program of China (2010CB934700), the Program of International S & T Cooperation (S2010GR0314), the National Natural Science Foundation of China (No. 50732006), and the Partner-Group of the Chinese Academy of Sciences-the Max Planck Society.

Supporting information for this article, including shear lag model analysis, Young's modulus of obtained films, synthesis of LDHs, Eu-Cl reinforced hybrid film, and characterization, is available on the WWW under <http://dx.doi.org/10.1002/anie.200906920>.



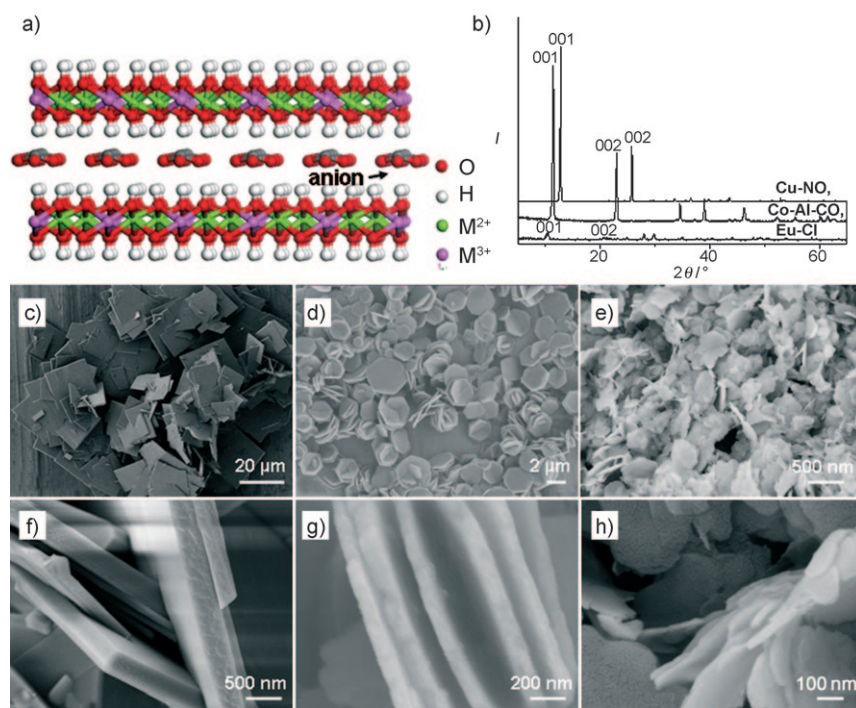


**Figure 1.** a) General crystal structure of LDHs. b) PXRD patterns of synthesized Cu-NO<sub>3</sub>, Co-Al-CO<sub>3</sub>, and Eu-Cl platelets. c–e) SEM images of synthesized Cu-NO<sub>3</sub> (c), Co-Al-CO<sub>3</sub> (d), and Eu-Cl platelets (e). f–h) SEM images of side views of Cu-NO<sub>3</sub> (f), Co-Al-CO<sub>3</sub> (g), and Eu-Cl platelets (h).

inorganic building blocks into a highly oriented 2D structure (Figure 2a). Then, an ethanol suspension containing 1 vol % modified LDH platelets was added dropwise onto the surface of deionized water. After ultrasonication, a smooth and perfectly oriented monolayer of platelets was formed at the air–water interface (Figure 2b). The assembled platelets were easily transferred to a glass substrate with a layer of chitosan (applied by spin coating) by simple dip coating because of strong hydrogen bonding between the amine-terminated silanes attached on the surface of the LDH platelets and the amine groups in the matrix of chitosan on the glass substrate (Figure 2c,d). The substrate was dried at 50 °C in an oven in ambient atmosphere, and then a new layer of chitosan was spin-coated onto the dried substrate (Figure 2e). Sequential repetition of these steps leads to multilayered organic–inorganic hybrid films with a total thickness of a few tens of micrometers. Free-standing colored transparent hybrid films were obtained by peeling off the films off the substrates with a razor blade (Figure 2f). The PXRD patterns of fabricated LDH–chitosan hybrid films (see the Supporting Information, Figure S1) indicate that the intrinsically layered symmetry of LDHs in the hybrid films is still kept, but with low crystallinity, and other diffraction peaks that appeared are possibly due to the influence of amine-terminated silane species and chitosan molecules on the LDHs.

It has been demonstrated that Cu-NO<sub>3</sub> and Co-Al-CO<sub>3</sub> platelets could assemble at the air–water interface, forming highly oriented monolayer 2D structures, when amine-terminated silane species were attached on their surfaces (Figure 3a–c). Three types of Cu-NO<sub>3</sub> and Co-Al-CO<sub>3</sub>

assemblies for fabricating LDH–chitosan hybrid films were designed: Type I: only Cu-NO<sub>3</sub> or Co-Al-CO<sub>3</sub> platelets were incorporated into the hybrid film (Figure 3e,f). Type II: Monolayers of Cu-NO<sub>3</sub> and Co-Al-CO<sub>3</sub> LDH platelets were alternately incorporated into the hybrid film (Figure 3g). Type III: The Cu-NO<sub>3</sub> and Co-Al-CO<sub>3</sub> LDH platelets were co-assembled at the air–water interface and then transferred to the substrate for the fabrication of the hybrid film (Figure 3h,i). The photographs in Figure 3 demonstrate that the hybrid films were all transparent and colored by the LDH platelets, and the color could be tuned by altering the combinations of LDH building blocks.

The cross-sectional microstructures of these hybrid films were investigated by SEM (Figure 4). For comparison, the pure chitosan film was fabricated by sequential LBL spin coating, but there is only one unit layer without lamellar microstructures inside this film (Figure 4a). By using LDH micro- and nanoplatelets as inorganic building blocks in LBL spin-coating procedures, the lamel-

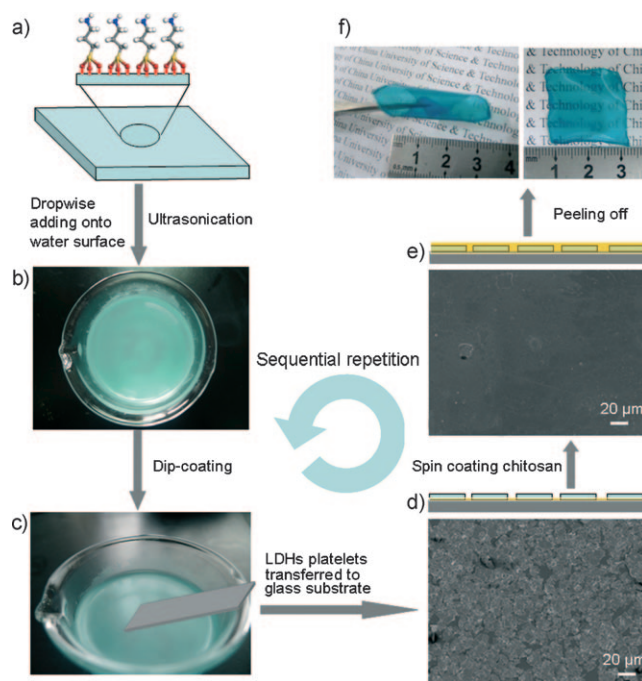


**Figure 2.** LBL bottom-up fabrication of multilayered LDH–chitosan hybrid films. a) Attachment of slightly hydrophobic amine-terminated silane species to the surfaces of LDH platelets. b) A highly oriented 2D monolayer of LDH platelets forms at the air–water interface by ultrasonication. c, d) Dip coating to transfer one layer of LDH platelets onto a glass substrate. e) Spin coating a new layer of chitosan on the LDH platelets. f) Photographs of the obtained free-standing Cu-NO<sub>3</sub>–chitosan hybrid film.

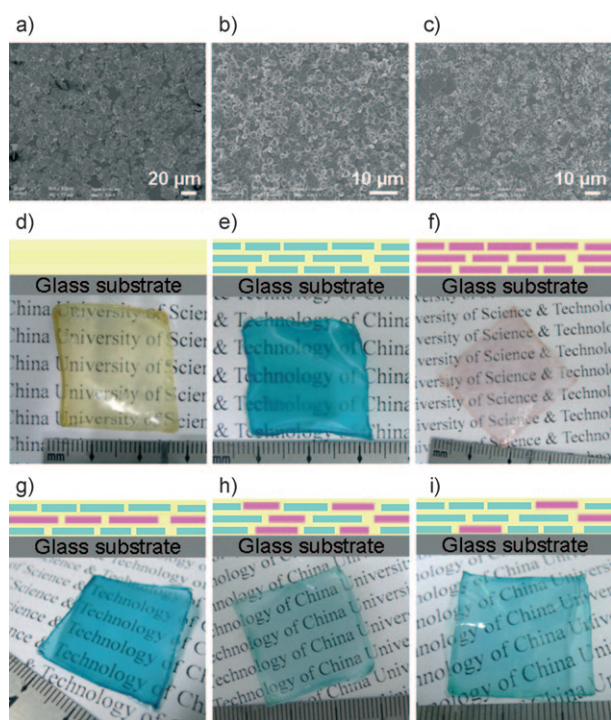


**Figure 3.** SEM images of 2D structures of LDH platelet assemblies at the air–water interface, fabricating models, and photographs of different films. a–c) SEM images of 2D structures of Cu-NO<sub>3</sub> (a), Co-Al-CO<sub>3</sub> (b), and V<sub>Cu-NO<sub>3</sub></sub>/V<sub>Co-Al-CO<sub>3</sub></sub> = 1:1 (c) platelets assembled at the air–water interface. d–i) Models and photographs of different films. d) Pure chitosan film. e) Cu-NO<sub>3</sub>-chitosan hybrid film. f) Co-Al-CO<sub>3</sub>-chitosan hybrid film. g) Alternating Cu-NO<sub>3</sub>-chitosan-Co-Al-CO<sub>3</sub>-chitosan hybrid film. h) Co-assembly V<sub>Cu-NO<sub>3</sub></sub>/V<sub>Co-Al-CO<sub>3</sub></sub> = 1:1-chitosan hybrid film. i) Co-assembly V<sub>Cu-NO<sub>3</sub></sub>/V<sub>Co-Al-CO<sub>3</sub></sub> = 3:1-chitosan hybrid film.

lar microstructures were incorporated into these hybrid films (Figure 4 b–d). Specifically, different 2D inorganic monolayers led to different micromorphologies of the hybrid films. This result indicates that the platelet-like LDH building blocks played a crucial role in the formation of lamellar microstructures that are similar to seashell nacre.

The tensile strength of fabricated films was measured to confirm the high strength of these hybrid films, which is thought to be brought about by the reinforcement effect of the inorganic LDH building blocks and by the biologically inspired layered microstructures. Figure 5a,b shows the tensile strength curves of pure chitosan film and of different LDH–chitosan hybrid films. The tensile strength of the hybrid films is much higher than that of the pure chitosan film, thus indicating that the LDH platelets reinforce the polymer matrix. It is worth mentioning that the tensile strength of the Cu-NO<sub>3</sub>-chitosan hybrid film reaches 160 MPa, thus making it stronger than some natural materials, such as nacre and dentin,<sup>[19]</sup> and almost eight times as strong as pure chitosan film. A simple shear lag model based on the mechanics of composite structures was proposed to explain the enhancement of tensile strength of the hybrid films by addition of LDH platelets in hybrid films.<sup>[11,20]</sup> In this model, the tensile strength of the hybrid film increases with an increase of the volume fraction ( $V_p$ ) of LDH platelets (see the Supporting

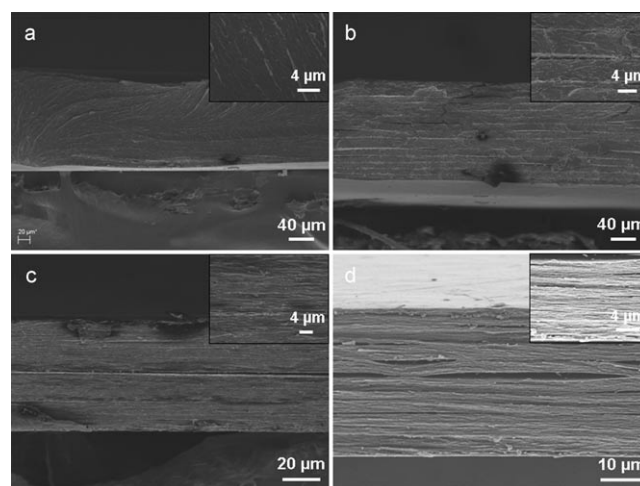


**Figure 4.** Cross-sectional SEM images of different films. a) Pure chitosan film (4 wt.% chitosan solution, spin coating at 1000 rpm). b) Co-Al-CO<sub>3</sub>-chitosan hybrid film (4 wt.% chitosan solution, spin coating at 1000 rpm). c) Alternative Cu-NO<sub>3</sub>-chitosan-Co-Al-CO<sub>3</sub>-chitosan hybrid film (3 wt.% chitosan solution, spin coating at 1000 rpm). d) Co-assembly 2D structure of V<sub>Cu-NO<sub>3</sub></sub>/V<sub>Co-Al-CO<sub>3</sub></sub> = 3:1-chitosan hybrid film (3 wt.% chitosan solution, spin coating at 1000 rpm). The inset images are magnifications.

Information, Part II). In our designed fabrication procedure, the  $V_p$  of LDH platelets in the hybrid films could be tuned by controlling the concentration of the chitosan solution and by using different co-assembly combinations of LDH platelets. Figure 5a shows that the tensile strength of Co-Al-CO<sub>3</sub>-chitosan hybrid films increases with a decreasing concentration of chitosan (a lower concentration of chitosan corresponds to a higher volume ratio of LDH platelets), which is consistent with the results of model analysis. Figure 5b shows that the tensile strength of hybrid films increases with the  $V_p$  of Cu-NO<sub>3</sub> platelets, which are larger and thicker than Co-Al-CO<sub>3</sub> platelets, thus further confirming the theoretical analysis that a higher volume fraction of platelets means higher tensile strength of the hybrid films. The Young's modulus of the hybrid films is also enhanced by an increase of LDH  $V_p$  (see the Supporting Information, Table S1), which further confirms the strength reinforcement induced by the LDH platelets and biologically inspired layered structure. The quite wide range of mechanical properties of obtained films (tensile strength from 20 to 160 MPa, Young's modulus from 2.3 to 12.7 GPa) is mainly due to the various compositions and fabrication types of obtained films.

The transparency for visible light of these fabricated films was investigated by light transmittance tests. Figure 5c shows 40–70 % transparence across the visible spectrum for Co-Al-CO<sub>3</sub>-chitosan hybrid films, in comparison with 50–90 % for a pure chitosan film. Figure 5d shows a very interesting result: the Cu-NO<sub>3</sub> hybrid films only allow visible light (400–600 nm) to pass through, thus indicating their potential application in special window materials protecting objects from being hurt by UV light. The nice visible-light transparence of hybrid films is attributed to the flat and uniform orientation of the LDH platelets in the hybrid films.<sup>[21]</sup> The light is not scattered



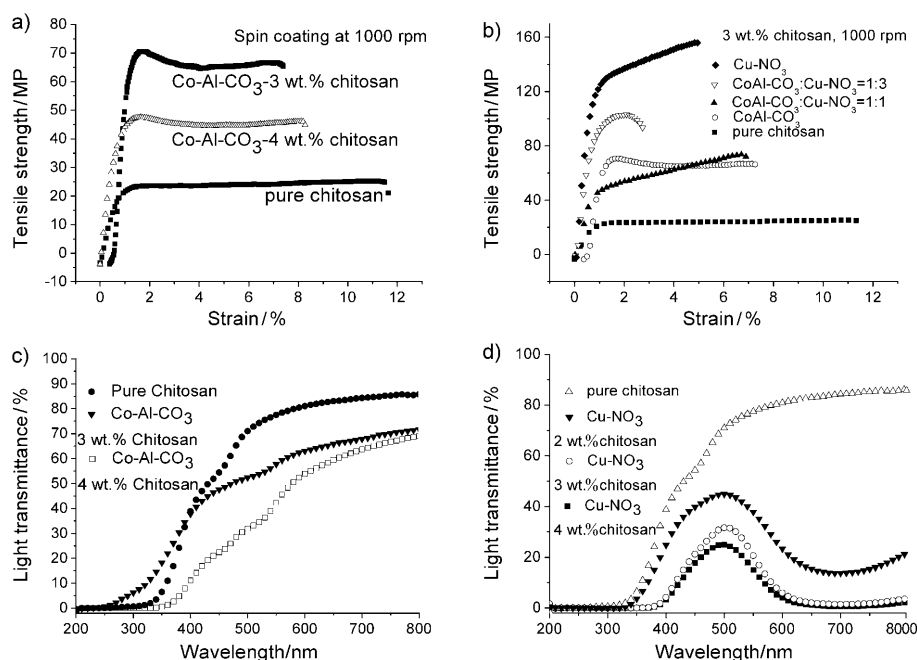


**Figure 5.** a) Tensile strength curves of Co-Al-CO<sub>3</sub>-chitosan hybrid films with different concentrations of chitosan comparison with pure chitosan film. b) Tensile strength curves of hybrid films with different 2D inorganic structures comparison with pure chitosan film. c) Light transmittance spectra of Co-Al-CO<sub>3</sub>-chitosan hybrid films comparison with pure chitosan film. d) Light transmittance spectra of Cu-NO<sub>3</sub>-chitosan hybrid films comparison with pure chitosan film.

by the sub-micrometer interfaces as in the original opaque powder form or many other composites with randomly dispersed LDHs.

A hybrid film with novel photoluminescent properties was also fabricated by using rare-earth-metal Eu-Cl nanoplatelets related to the LDHs as the functional building blocks (see the Supporting Information, Part III). It is interesting that the hybrid film not only emits red light but also emits blue light on irradiation with 360 nm light (see the Supporting Information, Figure S2a,b). The PL spectra analysis show that the blue light is caused by the chitosan matrix and that the red light comes from Eu-Cl (see the Supporting Information, Figure S2c). Furthermore, the tensile strength of the hybrid film is also enhanced compared with that of the pure chitosan film because of the inorganic platelets' reinforcement (see the Supporting Information, Figure S2d).

In summary, a series of free-standing, strong, transparent, and functional layered organic-inorganic hybrid films reinforced with LDH micro- and nanoplatelets can be fabricated through LBL assembly procedure using series of LDH platelets as building blocks. The microstructures and tensile strengths of these hybrid films have been investigated to show biologically inspired layered microstructures with high performance in mechanical properties. The tensile strength of the Cu-NO<sub>3</sub>-chitosan hybrid film achieved 160 MPa, which is eight times higher than that of a pure chitosan film and surpasses the strength of natural nacre. Furthermore, the Eu-Cl rare-earth nanoplatelets can also be used as building blocks for fabrication of light-emitting and strong films, which can emit red light under irradiation of 360 nm UV light and

maintain a fairly high strength. Further extension of the present strategy should allow access to a variety of high-quality hybrid thin films with tunable mechanical properties and multifunctionality by use of inorganic micro- and nanoplatelets with tunable thicknesses, sizes, and functionalities as building blocks.

## Experimental Section

**Materials:** Cupric nitrate (Cu(NO<sub>3</sub>)<sub>2</sub>·3H<sub>2</sub>O), aluminum chloride (AlCl<sub>3</sub>·6H<sub>2</sub>O), cobaltous chloride (CoCl<sub>2</sub>·6H<sub>2</sub>O), urea, europium oxide (Eu<sub>2</sub>O<sub>3</sub>), sodium chloride (NaCl), hexamethylenetetramine (HMT), chitosan, glacial acetic acid (CH<sub>3</sub>COOH), and absolute anhydrous ethanol were purchased from Shanghai Chemical Reagent Co. Ltd. Silane coupling agent 3-aminopropyltriethoxysilane (ATES) was purchased from YaoHua Co. Ltd. All chemicals were analytical grade and used as received without further purification.

**Synthesis of LDH platelet building blocks:** Micro- and nanoplatelets

of Cu<sub>2</sub>(OH)<sub>3</sub>NO<sub>3</sub>, [Co<sub>0.67</sub>Al<sub>0.33</sub>(OH)<sub>2</sub>][(CO<sub>3</sub>)<sub>0.165</sub>·0.49H<sub>2</sub>O], and Eu(OH)<sub>2.5</sub>Cl<sub>0.5</sub>·0.8H<sub>2</sub>O were synthesized according to reference [18a], [12a], and [18b], respectively. Details are given in the Supporting Information.

**Pretreatment of chitosan:** Chitosan (2, 3, or 4 g) was dissolved in deionized water (100 mL) containing 2 wt.% acetic acid. After the mixture had been vigorously stirred for one day, it was expected that the amine groups of chitosan were fully protonated by the acetic acid.

**Pretreatment of LDH platelets:** In a typical procedure, ATES (5 mL), methanol (12.5 mL), and deionized water (37.5 mL) were mixed and stirred for 1 h to completely hydrolyze the silane species. LDH platelets synthesized as described above were added to the mixture, which was then stirred for 5 min. (Note: Cu<sup>2+</sup> and the amine group of ATES can easily form a complex, so the mixture should not be stirred for longer than 5 min.) Finally, the silylated LDH platelets were filtered and washed several times with ethanol. The resulting LDH platelets were collected and redispersed in ethanol (30 mL).

**Fabrication of organic-inorganic hybrid films:** In a typical procedure, protonated chitosan (2, 3, or 4 wt.%; 1 mL) was dropped onto a 2.5 cm × 2.5 cm glass substrate, and then a spin coater (MODEL WS-400E-6NPP-LITE SHOWN, Laurell Technologies Corporation) was used to spin the substrate at 1000 rpm for 1 min to form a flat layer of chitosan. The substrate with one layer of chitosan was dried at 50 °C in an oven. The LDH platelets dispersed in ethanol were slowly dropped onto the water-air interface (a beaker was used to hold deionized water) until one visible layer of thin film formed; then the beaker was sonicated mildly for 15 min. After sonication, the LDH platelets form a compact inorganic layer. After finishing the two steps above, the glass substrate with chitosan was used to lift the inorganic thin film at the air-water interface through dip coating by hand. Then the film was dried at 50 °C. The procedure was repeated 10 to 20 times to fabricate films comprising 10 to 20 layers of inorganic platelets. Note: the first and last layer should always be chitosan. The obtained films should be placed in the oven

with high humidity, otherwise, the film will become brittle and the color of hybrid film will change after several tens of days in the dry air.

Received: December 8, 2009

Published online: February 24, 2010

**Keywords:** chitosan · layered compounds · organic–inorganic hybrid composites · thin films

- [1] a) I. A. Aksay, M. Trau, S. Manne, I. Honma, N. Yao, L. Zhou, P. Fenter, P. M. Eisenberger, S. M. Gruner, *Science* **1996**, 273, 892; b) G. Decher, *Science* **1997**, 277, 1232; c) A. Sellinger, P. M. Weiss, A. Nguyen, Y. Lu, R. A. Assink, W. Gong, C. J. Brinker, *Nature* **1998**, 394, 256.
- [2] G. Atlan, O. Delattre, S. Berland, A. LeFaou, G. Nabias, D. Cot, E. Lopez, *Biomaterials* **1999**, 20, 1017.
- [3] a) X. Li, W.-C. Chang, Y. J. Chao, R. Wang, M. Chang, *Nano Lett.* **2004**, 4, 613; b) J. Aizenberg, J. C. Weaver, M. S. Thanawala, V. C. Sundar, D. E. Morse, P. Fratzl, *Science* **2005**, 309, 275; c) K. J. Koester, J. W. Ager, R. O. Ritchie, *Nat. Mater.* **2008**, 7, 672.
- [4] a) R. K. Nalla, J. H. Kinney, R. O. Ritchie, *Biomaterials* **2003**, 24, 3955; b) F. Song, A. K. Soh, Y. L. Bai, *Biomaterials* **2003**, 24, 3623; c) R. K. Nalla, J. J. Kruzic, J. H. Kinney, R. O. Ritchie, *Biomaterials* **2005**, 26, 217; d) M. A. Meyers, P.-Y. Chen, A. Y.-M. Lin, Y. Seki, *Prog. Mater. Sci.* **2008**, 53, 1.
- [5] a) F. Barthelat, *Philos. Trans. R. Soc. A* **2007**, 365, 2907; b) N. Almqvist, N. H. Thomson, B. L. Smith, G. D. Stucky, D. E. Morse, P. K. Hansma, *Mater. Sci. Eng. C* **1999**, 7, 37.
- [6] a) J. Rexer, E. Anderson, *Polym. Eng. Sci.* **1979**, 19, 1; b) P. B. Messersmith, E. P. Giannelis, *Chem. Mater.* **2002**, 14, 1719; c) R. A. Schoonheydt, *Clays Clay Miner.* **2002**, 50, 411.
- [7] Z. Tang, N. A. Kotov, S. Magonov, B. Ozturk, *Nat. Mater.* **2003**, 2, 413.
- [8] P. Podsiadlo, A. K. Kaushik, E. M. Arruda, A. M. Waas, B. S. Shim, J. Xu, H. Nandivada, B. G. Pumphlin, J. Lahann, A. Ramamoorthy, N. A. Kotov, *Science* **2007**, 318, 80.
- [9] S. Deville, E. Saiz, R. K. Nalla, A. P. Tomsia, *Science* **2006**, 311, 515.
- [10] E. Munch, M. E. Launey, D. H. Alsem, E. Saiz, A. P. Tomsia, R. O. Ritchie, *Science* **2008**, 322, 1516.
- [11] L. J. Bonderer, A. R. Studart, L. J. Gauckler, *Science* **2008**, 319, 1069.
- [12] a) Z. P. Liu, R. Z. Ma, M. Osada, N. Iyi, Y. Ebina, K. Takada, T. Sasaki, *J. Am. Chem. Soc.* **2006**, 128, 4872; b) P. Gunawan, R. Xu, *J. Phys. Chem. C* **2009**, 113, 17206.
- [13] W. Kagunya, Z. Hassan, W. Jones, *Inorg. Chem.* **1996**, 35, 5970.
- [14] a) H. Zhang, K. Zou, H. Sun, X. Duan, *J. Solid State Chem.* **2005**, 178, 3485; b) D. G. Evans, X. Duan, *Chem. Commun.* **2006**, 485.
- [15] C. M. Jiao, Z. Z. Wang, Z. Ye, Y. Hu, W. C. Fan, *J. Fire Sci.* **2006**, 24, 47.
- [16] G. G. C. Arizaga, K. G. Satyanarayana, F. Wypych, *Solid State Ionics* **2007**, 178, 1143.
- [17] a) P. C. Pavan, L. P. Cardoso, E. L. Crepaldi, J. B. Valim, S. Abdelhamid, J. Mietek, *Stud. Surf. Sci. Catal.*, Vol. 129, Elsevier, New York, **2000**, pp. 443; b) W.-F. Lee, Y.-C. Chen, *J. Appl. Polym. Sci.* **2004**, 94, 2417; c) W. Chen, B. Qu, *Polym. Degrad. Stab.* **2005**, 90, 162; d) F. Costa, M. Saphiannikova, U. Wagenknecht, G. Heinrich in *Wax Crystal Control Nanocomposites Stimuli-Responsive Polymers*, **2008**, p. 101.
- [18] a) C. Henrist, K. Traina, C. Hubert, G. Toussaint, A. Rulmont, R. Cloots, *J. Cryst. Growth* **2003**, 254, 176; b) F. Geng, H. Xin, Y. Matsushita, R. Ma, M. Tanaka, F. Izumi, N. Iyi, T. Sasaki, *Chem. Eur. J.* **2008**, 14, 9255.
- [19] a) H. Sano, B. Ciucchi, W. G. Matthews, D. H. Pashley, *J. Dent. Res.* **1994**, 73, 1205; b) R. Z. Wang, Z. Suo, A. G. Evans, N. Yao, I. A. Aksay, *J. Mater. Res.* **2001**, 16, 2485.
- [20] A. P. Jackson, J. F. V. Vincent, R. M. Turner, *Proc. R. Soc. London Ser. B* **1988**, 234, 415.
- [21] a) L. Wang, C. Li, M. Liu, D. G. Evans, X. Duan, *Chem. Commun.* **2007**, 123; b) C. Li, L. Y. Wang, M. Wei, D. G. Evans, X. Duan, *J. Mater. Chem.* **2008**, 18, 2666.